



**HAL**  
open science

## Switchable Phase Transition from Crystalline to Amorphous States of Cadmium Sulfate Octahydrate Single Crystals by Shock Waves

Aswathappa Sivakumar, Sathiyadhas Sahaya Jude Dhas, Kondaveeti Showrilu, Paramasiva Sivaprakash, Raju Suresh Kumar, Abdulrahman I. Almansour, Shubhadip Chakraborty, Sonachalam Arumugam, Sathiyadhas Amalapushpam Martin Britto Dhas

► **To cite this version:**

Aswathappa Sivakumar, Sathiyadhas Sahaya Jude Dhas, Kondaveeti Showrilu, Paramasiva Sivaprakash, Raju Suresh Kumar, et al.. Switchable Phase Transition from Crystalline to Amorphous States of Cadmium Sulfate Octahydrate Single Crystals by Shock Waves. *physica status solidi (b)*, 2022, pp.2100662. 10.1002/pssb.202100662 . hal-03657582

**HAL Id: hal-03657582**

**<https://hal.science/hal-03657582>**

Submitted on 11 May 2022

**HAL** is a multi-disciplinary open access archive for the deposit and dissemination of scientific research documents, whether they are published or not. The documents may come from teaching and research institutions in France or abroad, or from public or private research centers.

L'archive ouverte pluridisciplinaire **HAL**, est destinée au dépôt et à la diffusion de documents scientifiques de niveau recherche, publiés ou non, émanant des établissements d'enseignement et de recherche français ou étrangers, des laboratoires publics ou privés.



Distributed under a Creative Commons Attribution - NonCommercial 4.0 International License

# Switchable Phase Transition from Crystalline – Amorphous States of Cadmium Sulfate Octahydrate Single Crystals by Shock Waves

A.Sivakumar<sup>1</sup>, S.Sahaya Jude Dhas<sup>2</sup>, K.Showrilu<sup>3</sup>, P. Sivaprakash<sup>4</sup>, Raju Suresh Kumar<sup>5</sup>,  
Abdulrahman I. Almansour<sup>5</sup>, Shubhadip Chakraborty<sup>6</sup>, S.Arumugam<sup>4</sup>, S.A.Martin  
Britto Dhas<sup>1\*</sup>

<sup>1</sup>Shock Wave Research Laboratory, Department of Physics, Abdul Kalam Research Center, Sacred Heart College, Tirupattur, Tamil Nadu, India – 635 601

<sup>2</sup>Department of Physics, Kings Engineering College, Sriperumbudur, Chennai, Tamilnadu, India - 602 117

<sup>3</sup>Department of Physics, Ch. S. D. St. Theresa College (A) for Women, West Godavari, Eluru, Andhra Pradesh, India- 534 003

<sup>4</sup>Centre for High Pressure Research, School of Physics, Bharathidasan University, Tiruchirapalli Tamilnadu, India - 620 024,

<sup>5</sup>Department of Chemistry, College of Science, King Saud University, P.O. Box 2455, Riyadh, Saudi Arabia- 11451

<sup>6</sup>Institut de Physique de Rennes, UMR CNRS 6251, Université de Rennes 1, 35042 Rennes Cedex, France

**Corresponding author:** [martinbritto@shcpt.edu](mailto:martinbritto@shcpt.edu)

## Abstract

Even slight changes occurring in the lattice positions of solid materials enforced by the external forces may give rise to remarkable results in the crystallographic nature. The materials which undergo phase - change without modifying their overall chemistry are the prominent candidates to be the driving forces for the applications involving phase transitions. In the present context, the authors present and demonstrate the switchable phase transition occurring between crystal-amorphous nature of cadmium sulfate octahydrate single crystals ( $3\text{CdSO}_4 \cdot 8\text{H}_2\text{O}$ ) impacted by shock waves with which the transition is authenticated via diffraction, vibrational and optical spectroscopic techniques such as powder X-ray diffractometry, Raman and UV – Visible spectral

This article has been accepted for publication and undergone full peer review but has not been through the copyediting, typesetting, pagination and proofreading process, which may lead to differences between this version and the [Version of Record](#). Please cite this article as [doi: 10.1002/pssb.202100662](https://doi.org/10.1002/pssb.202100662).

analyses. Based on the results attained from diffraction and spectroscopic analyses, it is observed that the switchable phase transition sequence is crystalline - crystalline - amorphous – crystalline - crystalline with respect to the control, one, two, three and four shock wave loaded conditions, respectively. Due to the outstanding switching behavior, the title material is strongly suggested for the applications of molecular switching and optical data storage systems.

**Key-words:** Shock waves,  $3\text{CdSO}_4 \cdot 8\text{H}_2\text{O}$ , switchable phase transition, re-crystallization

## Introduction

Pressure-driven shock waves emanating from in-house tabletop shock tubes have the profound potential to unlock a wide range of possible materials possessing peculiar properties which were previously inaccessible to many other testing methods so that an array of innovative pathways could possibly emerge materializing multidimensional scope for the materials science research wherein much of the demands of the industries can be met with, especially by the attainment of specific materials to meet the long-standing challenges. It has been a fascinating journey for the researchers to explore and understand the phase transition behavior of materials under shock wave loaded condition and it is one of the prominent research topics in recent years due to its technological predominance so that it is imperative to understand the behavior of materials. Any sudden release of energy in the form of pressure and temperature within few microsecond results in the formation of shock waves similar to the one generated at the moment of the explosion of bombs or volcanic eruption. If, such kinds of shock waves propagate through the materials, lots of structural deformations, structural transitions, defects, dislocations, re-crystallization effects may occur and these changes are highly associated with the nature of the materials as well as the structure of the materials.<sup>1-5</sup> In recent years, there have been several research articles published in this area especially in phase transitions such as crystalline to crystalline and crystalline to amorphous and amorphous to crystalline.<sup>6-9</sup> As far as it is known from the literature, attainment of the reversible phase transition behavior is comprehensively a critical task when compared to the irreversible transition influenced by shock waves.<sup>10-13</sup> Moreover, it could be noted that, so far several research articles have been published based on the shock wave induced phase transitions whereas the reversible phase transition of materials enforced by shock waves is not yet well understood. On the other hand, it is quite common to find materials at hydrostatic pressure compression and de-compression conditions which are well documented as exhibited by several materials such as acitamide<sup>14</sup>, Lithium amide<sup>15</sup>, Ammonium Formate<sup>16</sup> and magnesium silicide<sup>17</sup>. Reversible phase change (from amorphous to crystalline) materials are always given the prime importance as they have a wide array of technological applications such as switchable

dielectrics, thermal energy storage devices, piezoelectrics, ferroelectrics, pyroelectric as well as non-linear optical channel waveguides as compared to the phase changing materials of forward or backward phase transitions.<sup>18-20</sup> Moreover, in the last few decades, there are lots of research going on towards the understanding of the reversible phase change occurring in materials that are either crystalline – crystalline I- crystalline (CCC)<sup>14-17</sup> or crystalline – amorphous- crystalline (CAC)<sup>18-20</sup> achieved by various methods such as synthetic techniques and static high-pressure methods. Very recently, shock wave induced reversible phase changes such as crystallographic phase changes ( $K_2SO_4$ ) and magnetic phase changes ( $Co_3O_4$ ,  $ZnFe_2O_4$  and  $MnO_2$ ) have been observed by our group.<sup>21-25</sup>

From the literature survey, it is known that the hydrous metal (Mg, Ca, Cd, Ni and Fe) sulfates are better materials to exhibit reversible phase change behavior with respect to the exposed temperature, pressure and humidity. They are sensitive to the above-mentioned external parameters which have been very well documented and endorsed by the international scientific community.<sup>26,27</sup> The interesting behaviors of these materials are exhibited as and when they are in the hydrated state whereas they show the crystalline nature when they are in anhydride state wherein they transform to amorphous nature at a particular temperature and then they re-crystallize as crystalline materials on reaching the phase transition temperature which is quite common behavior for all the above-mentioned hydrate states of materials.<sup>28,29</sup> Vaniman et al. have demonstrated the transition of crystalline to amorphous and amorphous to crystalline occurring in  $MgSO_4$  with respect to temperature and humidity.<sup>29</sup> Moreover, understanding the stability of hydrated sulfate minerals at ambient conditions and non-ambient conditions is highly required to acquire a better understanding of planetary science and high pressure mineral science. These minerals are abundant and ubiquitous on the surface of the Earth, Mars and also on the other planets as well as on their respective satellites.<sup>26,27</sup>

Cadmium sulfate octahydrate ( $3CdSO_4 \cdot 8H_2O$ ) crystalline material is one of the important hydrate materials that are used in electroplating of cadmium in electronic circuits and as pigment in fluorescent screens. Quite a few researchers have published articles on  $CdSO_4 \cdot 8H_2O$  portraying crystal growth and their properties that have been recorded at ambient conditions.<sup>30,31</sup> Furthermore, the known polymorphic phases of the test sample are  $3CdSO_4 \cdot 8H_2O$  ( $C2/c$ ),  $CdSO_4 \cdot 4H_2O$ ,  $CdSO_4 \cdot H_2O$  ( $P2_1/c$ ) and  $CdSO_4$  ( $Cmcm$ ). The crystallographic structure of the title material was solved by Lipson<sup>32</sup> in 1936 and the crystal structure of  $CdSO_4 \cdot H_2O$  was re-determined by Chatphorn Theppitak et.al.<sup>33</sup> But, there are only a few publications on high-pressure and high-temperature that have been found for materials such as Mg, Ni and Fe hydrates. Hence,  $3CdSO_4 \cdot 8H_2O$  is a highly deserved material for shock wave impact analysis so as to understand better its structural stability

and structure – associated properties at extreme environmental conditions. Moreover, the title crystal belongs to the centrosymmetric nature and generally the centrosymmetric materials have a better probability to undergo reversible phase transition than that of the non-centrosymmetric materials because of their mirror symmetry.

In the present context, the authors present and demonstrate the switchable CAC phase transitions of  $3\text{CdSO}_4 \cdot 8\text{H}_2\text{O}$  by the influence of shock waves. To confirm the switchable CAC phase transitions, the results of diffraction and spectroscopic analyses are vital so that XRD, Raman and UV-Visible techniques have been performed to substantiate the observed phase transitions. It could be noted that no previous article is found, to date, on the title compound involving the high-pressure and high-temperature experiments. Hence, it is imperative to have the possible discussion on considering the similar work available on hydrate compounds and cadmium related compounds with their probable responses at high-pressure and high-temperature as well as shocked conditions.<sup>34-36</sup>

## **Experiential Section**

Commercially available  $3\text{CdSO}_4 \cdot 8\text{H}_2\text{O}$  compound (AR grade) was purchased so as to grow the test crystals to be used for the present experiment. The saturated solution of  $\text{CdSO}_4 \cdot 8\text{H}_2\text{O}$  was prepared using double distilled water at room temperature and stirred continuously for 5 h with the help of a magnetic stirrer in order to obtain a homogenous solution. Thereafter, the process of crystallization was allowed to take place by the slow evaporation method. After 40 days, bulk size  $3\text{CdSO}_4 \cdot 8\text{H}_2\text{O}$  crystals were harvested such that these crystals have been utilized for the analysis of phase transition impacted by shock waves. To start with, five crystals of (402) plane have been selected with equal dimension ( $10 \times 10 \times 1 \text{mm}^3$ ) for this study. One sample has been kept as the control and the remaining four samples have been sent for shock wave impact study. The working methodology and shock wave loading procedure of the shock tube used for the investigation have been discussed in our earlier publications.<sup>22,37</sup> In the present experiment, shock waves of Mach number 2.2 have been utilized with the transient pressure and temperature of one shock pulse as 2.0 MPa and 864 K, respectively. The four test samples have been subjected to shock waves such that 1, 2, 3 and 4 shock pulses have been loaded, respectively with a regular time interval of 5 seconds between the shock pulses and the impact of shock waves on the test crystal has been screened by diffraction and spectroscopic techniques.

## **Results and Discussion**

### **XRD analysis**

Powder X-ray diffraction technique has been employed to analyze the crystallographic structure of the test crystal and the crystallographic nature of the test samples at shocked conditions. Fig.S1, (ESI) shows the single molecular configuration and unit cell packing of the test crystal (generated from CIF file). On the one hand, the water molecules are highly sensitive in these kinds of metal hydrate crystals even at lower temperatures which can be removed from the original crystal structure so that lower hydrate compounds are produced.<sup>35</sup> On the other hand, mixed phase can coexist even at 25-30°C and  $\text{MgSO}_4 \cdot 7\text{H}_2\text{O}$  is one of the best examples for the formation of mixed phase.<sup>34,35</sup> Hence, substantiation of the grown crystal structure is highly valid.

A comparison is made between the diffraction patterns of the control crystal and the simulated XRD pattern of the title crystal such that the corresponding XRD patterns are presented in Fig.1. As seen in the XRD pattern of the control, it has a very strong diffraction peak at 33 degree and its corresponding plane orientation is (402). In the higher angle region, one more considerable diffraction peak is observed at 46.1 degree and its corresponding plane orientation is (060). Moreover, two more diffraction peaks are also observed and the corresponding diffraction peaks are (22-2) and (353), but they have less peak intensity. In the ideal case of a single crystal, there should be a single diffraction peak while recording the diffraction profile. But, due to the presence of defects, deformations and multiple growth directions, there might be a possibility for a couple of tiny peaks wherein these kinds of multiple growths might have occurred such that grain growths are uncontrollable in crystals grown by slow evaporation technique.<sup>38</sup>

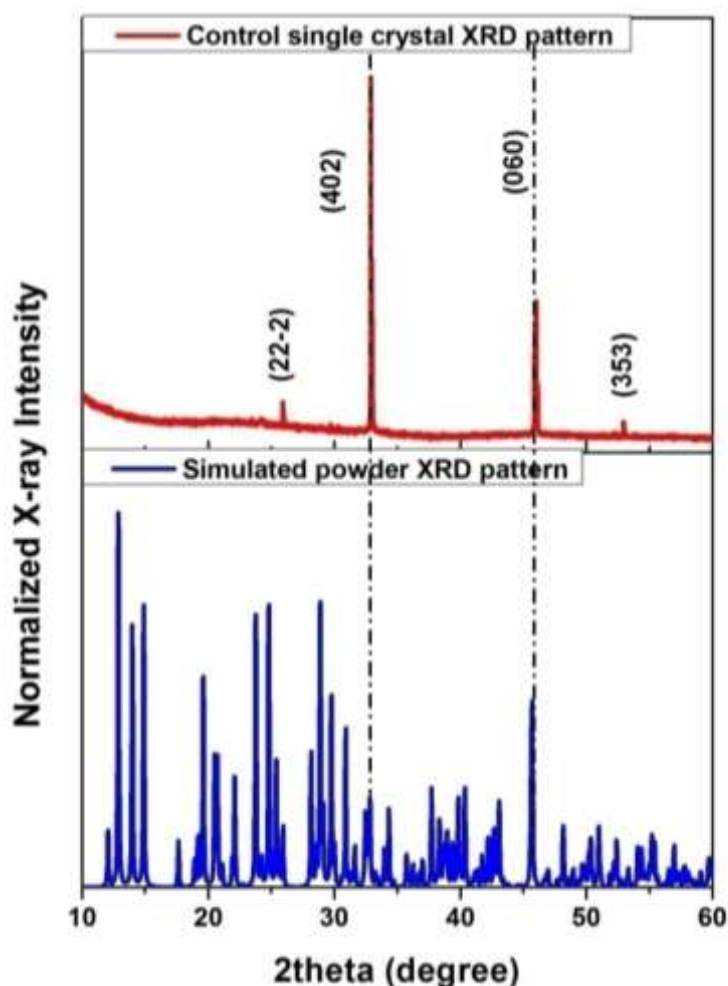


Fig.1 XRD patterns of simulated and the control crystals of  $3\text{CdSO}_4 \cdot 8\text{H}_2\text{O}$

Hence, a couple of strong diffraction peaks as well as minor diffraction peaks are observed. But, all the diffraction peaks observed are found to be well-matched with the XRD pattern of the simulated test sample and JCPDS card No; 75-2081. Therefore, it is confirmed that the test crystal has the monoclinic structure and  $C2/C$  space group and the lattice dimensions are found to be  $a=14.7928 \text{ \AA}$ ,  $b=11.8921 \text{ \AA}$ ,  $c=9.4581 \text{ \AA}$  and  $V= 1650.08 \text{ \AA}^3$  and the observed values are well corroborated with Lipson and Ruggero Caminiti reports [32,33]. As per the crystal structure of  $3\text{CdSO}_4 \cdot 8\text{H}_2\text{O}$ , it has the typical cation octahedral coordination geometry which is surrounded by four oxygen centers contributed by four sulfate ligands and two oxygen centers from the bridging water molecules and the anion  $\text{SO}_4$  has tetrahedral coordination as well as it has one free water molecule. The crystallographic structural stability of the test crystal is mainly based on the network of the corner linkage of  $\text{CdO}_4(\text{H}_2\text{O})_2$  octahedral and  $\text{SO}_4$  tetrahedral in addition to the strengthening of hydrogen bonds. In the case of the test crystal, it has two lattice sites such as special positions and general positions site symmetry. The atoms such as Cd(2) and S(1) are located at special positions site symmetries -1 and 2, respectively. All the remaining atoms are located at general

positions site symmetry.  $3\text{Cd}^{2+}$  is a soft cation surrounded by 8  $\text{H}_2\text{O}$  molecules since the hydrogen bonds in the water molecules are very weak. On the other hand,  $\text{CdO}_4(\text{H}_2\text{O})_2$  octahedral is not an ordinary octahedral such that it cannot be compared with other octahedral coordination structures since the atoms comprising the groups in this case are not in contact.<sup>32,39</sup> Such kind of weak hydrogen bonds and corner sharing octahedral and tetrahedral coordination bonds may play a significant role in the external conditions and the effect of shock waves on crystal structure are discussed in the following sections.

XRD patterns of the shocked crystals are presented in Fig.2 wherein significant changes have been observed with respect to the number of shock pulses. As seen in Fig.2, the strong diffraction peak identified at 33.00 degree has experienced a higher angle shift to 33.48 degree and hence the crystal orientation is also changed from (402) to (511) at the 1<sup>st</sup> shocked condition. On the other hand, the second strong diffraction (060) has completely disappeared at the 1<sup>st</sup> shocked conditions and a new diffraction peak appears at 29.02 degree and this diffraction position belongs to (312) crystal plane. On the other hand, a few of lower as well as higher angle minor diffraction peaks are found to have completely disappeared. These changes may be due to the re-orientation of grains in the test crystal by the impulsion of shock waves and similar results have been observed in potassium dihydrogen phosphate (KDP) powder sample at shocked conditions with respect to the number of shock pulses.<sup>40</sup> In the case of KDP samples, the diffraction peak (204) has completely disappeared at 50 shocks and re-appeared at 100 shocks pulse loaded conditions. On the other hand, diffraction peak (324) has appeared newly at 50 shocked conditions due to the occurrence of dynamic re-orientation of grains. Here also, the similar behavior is observed which justifies the observed results at shocked conditions. Changes occurring in the water molecule positions and its orientations are bound to be with high possibility at shocked conditions due to its lower bond energies. In addition to that, during the shock wave loaded conditions, polyhedral linking angle might have changed that could also contribute to the orientational changes in the crystal structure. Moreover,  $\text{CdO}_4(\text{H}_2\text{O})_2$  octahedral and  $\text{SO}_4$  tetrahedral also have the partial contribution in the observed orientational changes. Since  $\text{CdO}_4(\text{H}_2\text{O})_2$  octahedral sites have undergone tilting,  $\text{SO}_4$  tetrahedral sites are highly free for rotational order–disorder process at high-pressure and high-temperature conditions.<sup>41,42</sup> Hence, such kind of re-orientational changes are quite usual to occur at shocked conditions in sulfate materials.<sup>21</sup> It could be noted that, at this stage, the test sample has not undergone any crystallographic phase transitions and lower hydrate formation. It is worthwhile to mention here that, as per the previous article,  $\beta\text{-K}_2\text{SO}_4$  to  $\alpha\text{-K}_2\text{SO}_4$  crystal phase transition has been observed at one pulse of shock wave loaded condition due to the existence of the rotational disorder



of  $\text{SO}_4$  tetrahedral.<sup>21</sup> But here, such kind of significant changes are not observed which may be due to the presence of hydrogen bonds in the crystal system.

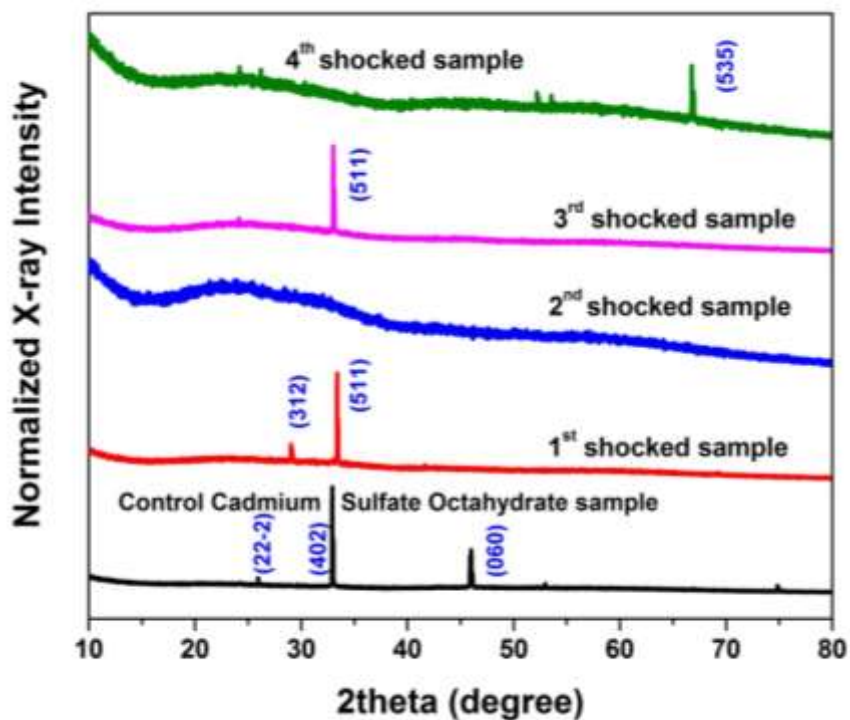


Fig.2 XRD patterns of the control and shocked  $3\text{CdSO}_4 \cdot 8\text{H}_2\text{O}$  samples

At the 2<sup>nd</sup> shocked condition, none of the crystalline peak is visible, not even the minor crystalline peaks. Hence, it is considered as an amorphous phase which may be due to the collapse of the long-range order of  $3\text{CdSO}_4 \cdot 8\text{H}_2\text{O}$  crystal. During the shock wave loaded condition, amorphization of crystalline solids has been reported in carbon boride<sup>43</sup>, ZIF-8<sup>1</sup> and mullite<sup>44</sup>. In the present case, the amorphization of the test crystal may be due to the existence of lattice - disorder in coordination water molecules in the octahedral site or breaking of water molecules bonds from the octahedral coordination. In the test crystal structure, the water molecules are included to fill up the interstices in the structure and it appears that, under these circumstances, the dispositions of the bonds can be greatly distorted from their mean position and tetrahedral nature.<sup>32</sup> There are four independent water molecules in the crystal structure in which only one oxygen atom (O10) is not bonded with the cadmium. The arrangement around O10 is approximately tetrahedral. It forms two hydrogen bonds with sulfate oxygen's O1 and O5 and accepts two bonds from two water molecules coordinated with Cd (O9 and O7). Cd-O from sulfate group is 2.287 Å and the bond length between Cd and S is 3.430 Å.<sup>39</sup> Hence in water molecules, the hydrogen bonds have the first possibility to break away and deform the hydrogen bonds. On the other hand,  $\text{SO}_4$  tetrahedral always prefer order-disorder process with respect to pressure and temperature and the bond length between S and

O atoms in the tetrahedral site is 1.475 Å. All oxygen atoms of the sulfate groups are bonded to different cadmium ions, thus joining them into the three-dimensional network. However, it is very clear that, if one bond is broken, the entire octahedral and tetrahedral sites may have to experience a significant collapse of the entire long-range order of atomic arrangement in the crystal and it induces the structural destabilization without changing the actual chemistry of the crystal. Such kind of changes may happen in the present case of 2<sup>nd</sup> shocked condition. Hence at the shocked condition, the degree of distortion may be significantly increased in such a way that the formation of an amorphous phase is enforced and it can be called as dynamic re-crystallization.<sup>43</sup> As per the earlier publications, several metal salts of hydrate materials have experienced the amorphization during the high-temperature and high-pressure experiments which is based on the de-hydration process.<sup>34-36</sup> But, in the present case, such kind of de-hydration process has not appeared since the crystal remains to be in its original colour (colourless) after the second shock wave loaded condition. Hence, it is strongly believed that the water molecules do not come out of the crystal. It could be noted that, without the loss of water molecules, amorphization is highly rare as compared to the amorphization caused by de-hydration process.<sup>34-36</sup> Furthermore, the present experimental investigation has been extended in terms of number of shocks with respect to crystallographic phase of the test sample which could give a possible better understanding about the crystal structure at shocked conditions. Hence, 3<sup>rd</sup> and 4<sup>th</sup> shocked conditions have been enabled for the respective crystals and the observed XRD patterns are presented in Fig.2. Surprisingly, a strong and intense diffraction peak (511) is noticed at 33.48 degree at the 3<sup>rd</sup> shock wave loaded condition. Hence, at this stage, it is confirmed that the amorphous phase of the test crystal is transformed to the crystalline phase which is found to be an unusual behavior at shocked conditions and the interesting thing is that the observed diffraction peak (511) belongs to C2/C crystal phase of the test sample. In Fig.4, it is shown the projection of (402), (511) and (535) planes with c-axis and the red balls indicate the non-bonded water molecules.

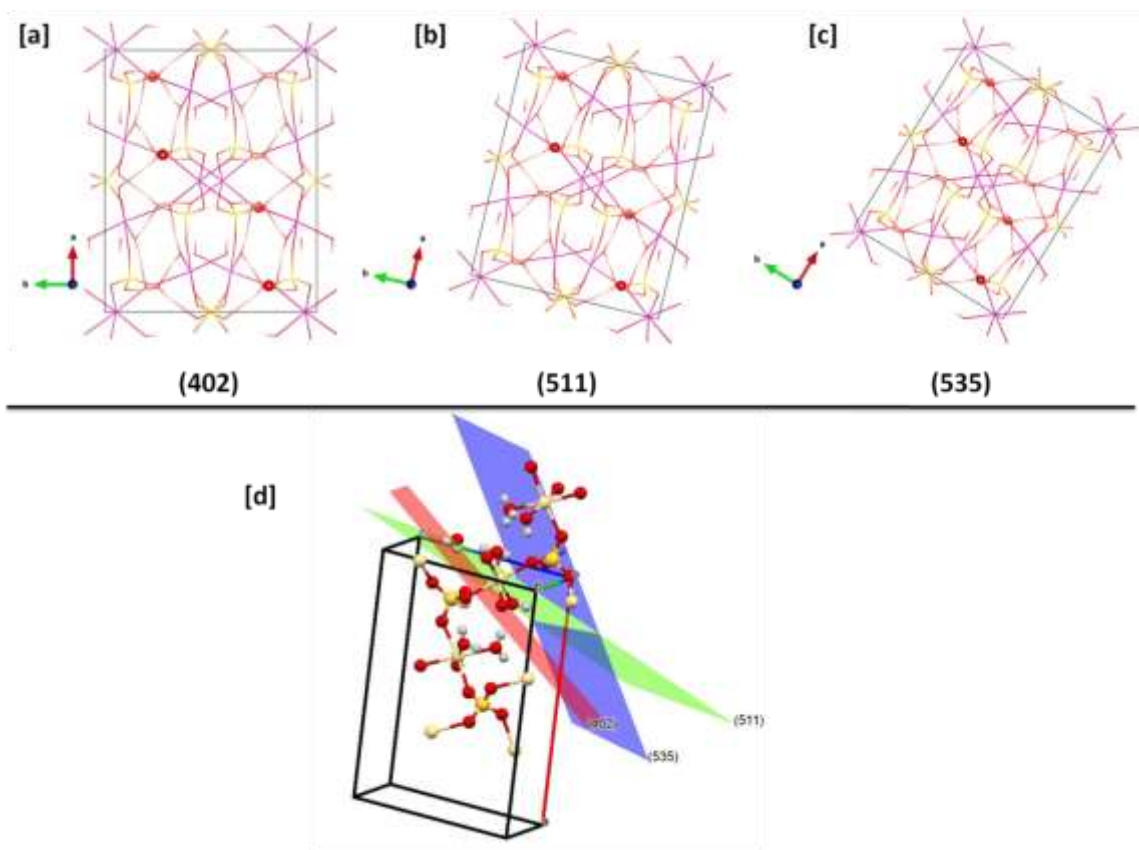


Fig.3 Packing of the molecules in [a] (402), [b] (511) and [c] (535) planes of the test crystal along c-axis [d] Unit cell packing of the observed major three planes

At this stage, on analyzing how a complete disordered system could become an ordered system at shocked conditions, it is essential to bring in a couple of concepts such as hot spot nucleation mechanism (dynamic re-crystallization process) and rotational order-disorder behavior of  $\text{SO}_4$  tetrahedral. As per the hot spot nucleation mechanism, during the shock wave loaded conditions, a sufficient latent heat is supplied to the crystal system. Due to the latent heat, the disordered system can be turned into the ordered system and the resultant phase transition from amorphous to crystalline nature could be accomplished.<sup>9,21</sup> Furthermore, as  $\text{SO}_4$  tetrahedral is sensitive for pressure and temperature, it is induced by the rotational order – disorder and vice versa.<sup>21</sup> In the case of  $\text{K}_2\text{SO}_4$  crystal, it shows the highly disordered  $\alpha$ -phase at the 1<sup>st</sup> shocked condition and the observed XRD pattern looks like semi-crystalline. But at the 2<sup>nd</sup> shocked condition, the complete crystalline nature is observed which is due to the occurrence of rotational disorder- order of  $\text{SO}_4$  tetrahedral.<sup>21</sup> Similar behaviour might have happened in the present case as well so that amorphous to crystalline phase transition has occurred at the 3<sup>rd</sup> shocked condition. All the  $\text{SO}_4$  tetrahedral connected with a couple of hydrogen bonding may easily be crystallized when supplied with the sufficient latent heat.<sup>9,21,28</sup> At the 4<sup>th</sup> shocked condition, the test crystal exhibits a few of minor diffraction peaks whereas a strong diffraction peak appears at 66.80 degree for which

the corresponding crystal orientation is (535). The formation of minor diffraction peaks may be due to the breaking of single grains influenced by the impact of shock waves so that the dynamic lattice plane re-orientation might have occurred. Here also, there is no signature found for de-hydration by the impact of shock waves and all the diffraction peaks observed belong to  $C2/c$  phase diffraction planes of the test crystal. The phase profile of the test crystal with respect to the number of shock pulse is presented in Fig.4.

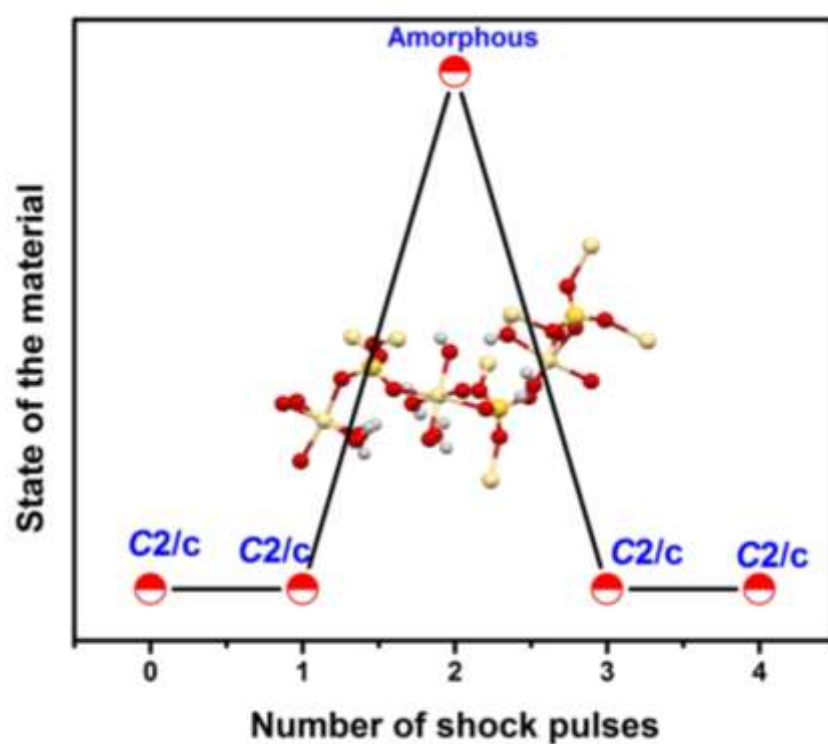


Fig.4 Phase profile of the test crystal with respect to the number of shock pulses

### Raman spectral Analysis

Raman spectral analysis has been performed to understand better the switchable phase transition of the test crystal in spectroscopic point of view as it is one of the prime tools to study the structures of water such that it can give accurate characteristic spectroscopic signal for intramolecular O–H valence bonds. The test crystal is highly associated with water molecules and the contribution of water molecules in the observed structural changes of the test crystal at shocked conditions has to be considered for making the clear picture about the structural changes. Hence, Raman spectral analysis has been performed. Raman spectra have been recorded over the wavenumber region of 50-3500  $\text{cm}^{-1}$  and the obtained Raman spectra of the control and shocked crystals are presented in Fig.5. As seen in the Raman spectrum of the control crystal, the characteristic peaks of  $\text{SO}_4$  are observed at 453  $\text{cm}^{-1}$ , 622  $\text{cm}^{-1}$ , 1004  $\text{cm}^{-1}$ , and 1113  $\text{cm}^{-1}$  for  $\nu_2$ ,  $\nu_4$ ,

$\nu_1$ , and  $\nu_3$ , respectively. Furthermore, the water band position is observed at  $3423\text{ cm}^{-1}$  and all the observed Raman band positions are well corroborated with the results of previous publication of the test crystal.<sup>31</sup> As seen in Fig.5, all the Raman bands have the same positions with respect to the number of shock pulses. It is provided a few Raman bands with the zoomed-in versions in Fig.6 so as to visualize the impact of shock waves on the test crystal. While looking into the zoomed-in Raman spectra, significant changes have been observed such as Raman shift and Raman intensity in  $\text{SO}_4$  ( $\nu_2$ , and  $\nu_3$ ) and Raman bands of hydrogen bonds. The  $\nu_4$ , and  $\nu_1$  of  $\text{SO}_4$  Raman bands remain the same with respect to the number of shocks. In Fig.6, zoomed-in version is provided for the  $\text{SO}_4$  characteristic peaks of  $\nu_2$ ,  $\nu_4$ ,  $\nu_1$ , and  $\nu_3$  and the corresponding Raman bands are presented.

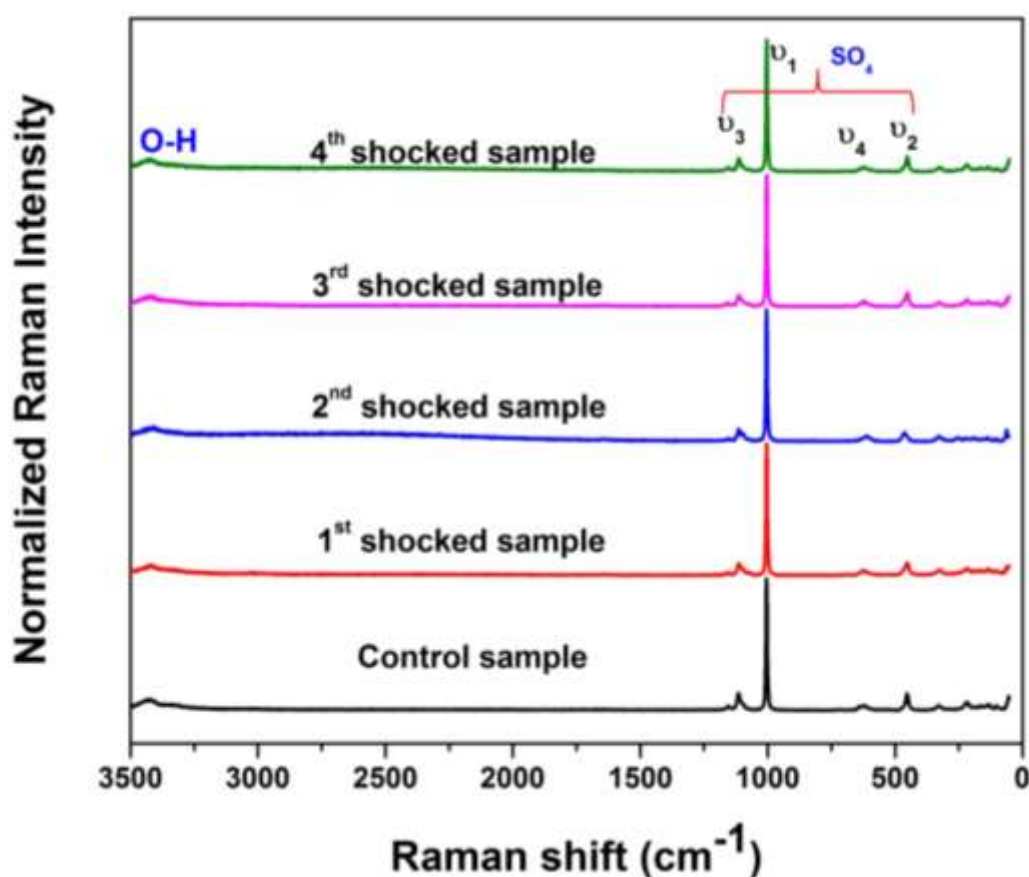


Fig.5 Raman spectra of the control and shocked  $3\text{CdSO}_4 \cdot 8\text{H}_2\text{O}$  samples

As seen in Fig.6a, the characteristic Raman band of  $\text{SO}_4$  ( $\nu_2$ ) is present at  $453\text{ cm}^{-1}$  which has moderate Raman intensity such that it belongs to the symmetric stretching vibration of  $\text{SO}_4$  tetrahedral. At the 1<sup>st</sup> shocked condition, similar Raman band is reproduced in terms of Raman band position and intensity. At the 2<sup>nd</sup> shocked condition, the Raman band position is shifted towards higher wavenumber i.e.  $453\text{ cm}^{-1}$  to  $462\text{ cm}^{-1}$  (blue shift:  $\sim 9\text{ cm}^{-1}$ ) and the observed shift may be due to the existence of the amorphization of the test crystal. Similar kind of blue shift of  $\text{SO}_4$  band is

observed in the amorphization of  $\text{MgSO}_4 \cdot 7\text{H}_2\text{O}$  at high pressure compression and high temperature experiments.<sup>45</sup> Usually, such kind of Raman shifts of  $\text{SO}_4$  bands occur during the deformation and disorder of  $\text{SO}_4$  tetrahedral sites in the crystal structure and it has been very well documented.<sup>21,45</sup>

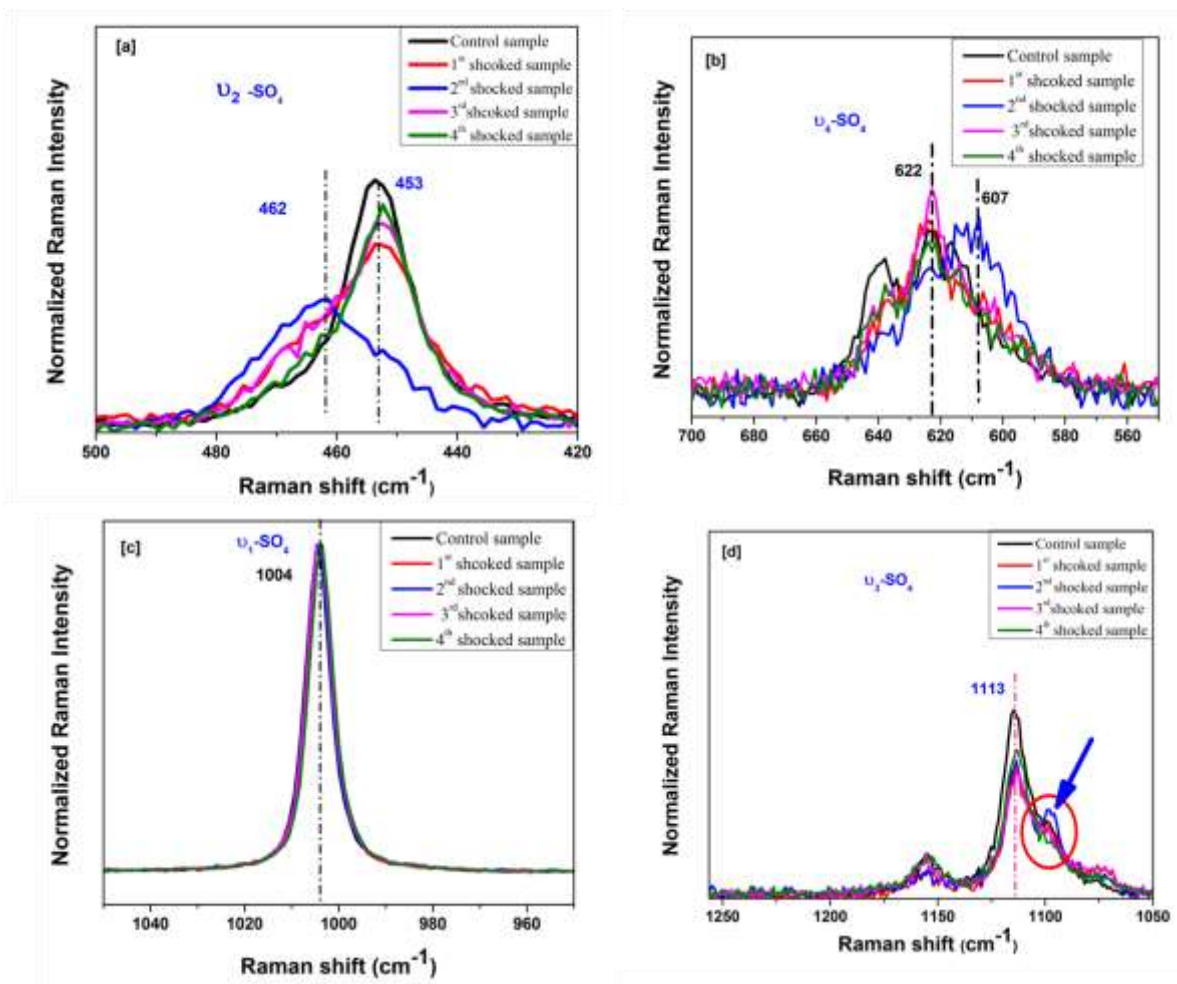


Fig.6 Zoomed-in versions of Raman spectra of the control and shocked samples (a)  $420\text{-}500\text{ cm}^{-1}$  (b)  $550\text{-}700\text{ cm}^{-1}$  (c)  $950\text{-}1050\text{ cm}^{-1}$  (d)  $1050\text{-}1250\text{ cm}^{-1}$

In the crystal structure of the sample, four independent water molecules (O10) are present per unit volume and they are shown in Fig.3a with red balls. Hence, it is very clear that, three of these hydrogen bonds are connected with  $\text{CdO}_6$  octahedral and one hydrogen bond is connected with sulfate oxygen.<sup>32</sup> Furthermore, the test crystal has 12 hydrogen bonds per unit volume and a few hydrogen bond details are listed that are associated with free water molecules (Fig.7).<sup>32</sup> The formation of hydrogen bonds between the free water molecular structures are  $\text{O7}\text{---}\text{H1}\cdots\text{O2}$  ( $2.973\text{ \AA}$ ),  $\text{O10}\text{---}\text{H7}\cdots\text{O2}$  ( $2.973\text{ \AA}$ ) and  $\text{O10}\text{---}\text{H8}\cdots\text{O1}$  ( $2.840\text{ \AA}$ ). It could be noted that, the above-mentioned bond lengths are quite larger than the actual coordination groups ( $2\text{ \AA}$ ).<sup>32</sup> Due to higher hydrogen bond lengths, it may undergo bond breaking at the second shocked condition and induce the lattice disorder which results into the formation of amorphization. Note that, at this stage, the

hydrogen bond network of the test crystal is completely varied and the changes occurring in hydrogen bond network will be discussed in next section. The other sulfate Raman bands of  $\nu_3$  and  $\nu_4$  also give the possible substantiations to justify the re-organization of hydrogen bonds at the 2<sup>nd</sup> shocked conditions.  $\nu_4$  Raman band undergoes red shift and  $\nu_3$  Raman band shows the formation of shoulder peak at higher wavenumber that are presented in Fig.6b and Fig.6d. These observed changes may be due to the amorphization of the test crystal at the second shocked condition. But, it could be noted that, among all sulfate Raman bands such as  $\nu_1$ ,  $\nu_2$ ,  $\nu_3$  and  $\nu_4$ , only at the 2<sup>nd</sup> shocked condition, the Raman band positions and intensities change significantly and it corresponds to the possible agreement with the XRD results.

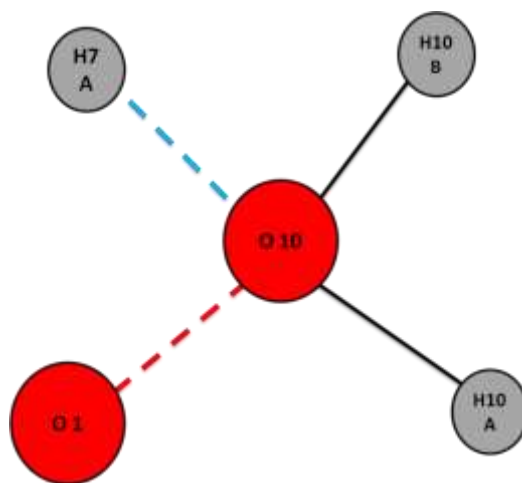


Fig.7 Free water molecular structure of the test crystal

Followed by the Raman bands corresponding to sulfate, the investigation of the Raman bands of hydrogen bonds and water molecular bands are highly crucial since the observed structural changes are highly associated with the re-organization of hydrogen bonds and the corresponding Raman bands are presented in Fig.8. As seen in Fig.8a, the Raman band takes place at  $222\text{ cm}^{-1}$  in the control crystal and it is considered to be associated with hydrogen bonding in the structural unit of the test crystal.<sup>46</sup> The Raman bands of hydrogen bond positions and intensities are nearly similar for the control, 1<sup>st</sup>, 3<sup>rd</sup> and 4<sup>th</sup> shocked conditions and this is the non-debatable proof which justifies the above-mentioned shocked crystals having the same crystalline nature with same crystallographic phase (C2/C). The significant higher wave-number shift has been observed from  $222\text{ cm}^{-1}$  to  $256\text{ cm}^{-1}$  at the 2<sup>nd</sup> shocked condition and this significant Raman shift may be due to the re-organization of hydrogen bonds which may lead to the progressive breakdown of lattice symmetry that enhances the lattice disorder of the test crystal.<sup>45</sup> With respect to this lattice disorder, Cd1 and Cd2 may exhibit a distorted octahedral coordination which breaks the lattice symmetry of the test crystal and induce the formation of amorphization at the 2<sup>nd</sup> shocked

condition. In Fig.8b, the water molecular Raman bands of the control and shocked crystals are presented and this region is highly crucial followed by the region of hydrogen bonds. Since, as per the previous reports on high-pressure and high-temperature experiments, amorphization of minerals has been observed during the de-hydration process which has been well documented by the materials and mineral scientists.<sup>34,36</sup> If such kind of de-hydration process has been undergone by the test crystal it might have turned into milky white that has been well documented for several standard minerals such as  $\text{MgSO}_4 \cdot 7\text{H}_2\text{O}$  and  $\text{CuSO}_4 \cdot 5\text{H}_2\text{O}$ .<sup>35,47</sup> The water molecular Raman bands of the control and shocked crystals are presented in Fig.8b. In the case of the control crystal, the water molecular (O-H bond) Raman band position is observed at  $3423 \text{ cm}^{-1}$  which is found to be very well corroborated with the earlier publications.<sup>45</sup> Interestingly, here also similar changes are observed as that of Raman bands of sulfate ion  $\nu_4$ . As seen in Fig.8b, the control, 1<sup>st</sup>, 3<sup>rd</sup>, and 4<sup>th</sup> shocked crystal's Raman band position of water remains the same. But at the second shocked condition, the Raman band is shifted towards the lower wave-number from  $3423 \text{ cm}^{-1}$  to  $3409 \text{ cm}^{-1}$  which clearly indicates the re-organization of hydrogen bonds and enforces changes in the bond lengths that represent the change in the bonding pattern of crystal lattice which might have induced the amorphization at the 2<sup>nd</sup> shocked conditions.<sup>48</sup>

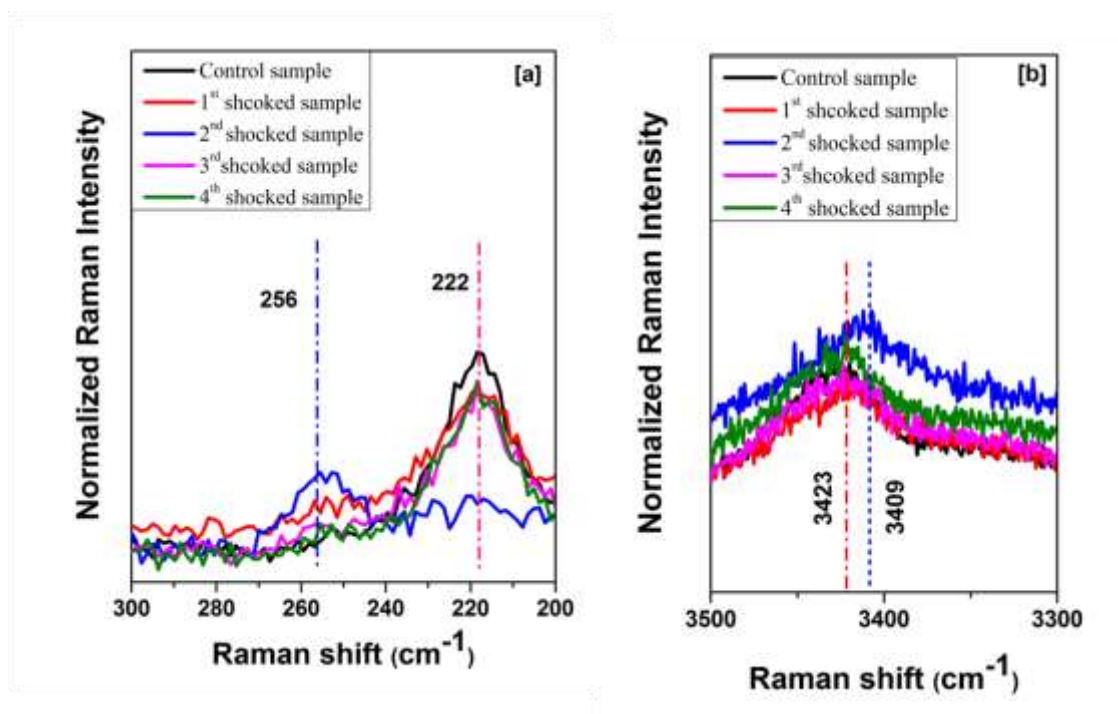


Fig.8 Raman bands of hydrogen bonds and water bonds of the control and shocked samples

Furthermore, in Fig.9, the lattice mode vibration Raman bands of the control and shocked crystal are presented. Usually,  $10\text{-}200 \text{ cm}^{-1}$  Raman bands are considered as the lattice modes such that lattice mode vibrations are observed at  $62 \text{ cm}^{-1}$ ,  $72 \text{ cm}^{-1}$ ,  $101 \text{ cm}^{-1}$ ,  $136 \text{ cm}^{-1}$  and  $166 \text{ cm}^{-1}$  for



the control crystal whereas significant changes are observed in lattice mode vibration of the test crystal at the 2<sup>nd</sup> shocked conditions. But for the remaining shocked conditions, the lattice mode positions are similar at the 2<sup>nd</sup> shocked condition. But, the lattice mode vibrations such as 72 cm<sup>-1</sup> and 166 cm<sup>-1</sup> have completely disappeared which is shown in red circles in Fig.9 and it may be due the existence of the amorphization.

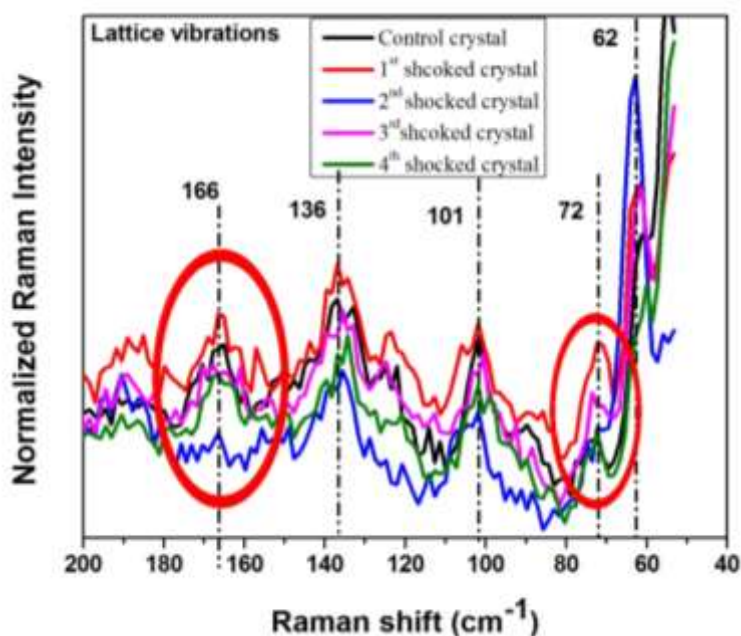


Fig.9 Lattice mode vibrations of the control and shocked samples

### UV-Visible spectral Analysis

In recent years, much attention has been paid to understand the impact of shock waves on optical properties of optically transparent materials. Moreover, the impact of shock waves on optical properties is less understood as compared to the crystallographic phase stability aspects. As per the results of recent publications, optical properties such as optical transmittance and absorption edges of both bulk and nano-materials are significantly altered with respect to the number of shock waves.<sup>21,22,49-53</sup> Hence, in the present work, as per the XRD and Raman spectral results, investigation of optical properties is highly required since it is an optically transparent crystal such that it could provide scope for better justifying the obtained changes through diffraction and vibrational spectral results of the test crystal at shocked conditions. Varian carry 5E UV-Visible spectrometer has been utilized to assess the optical transmittance of the test crystal at shocked conditions and the recorded optical transmittance profiles of the crystals are presented in Fig.10.

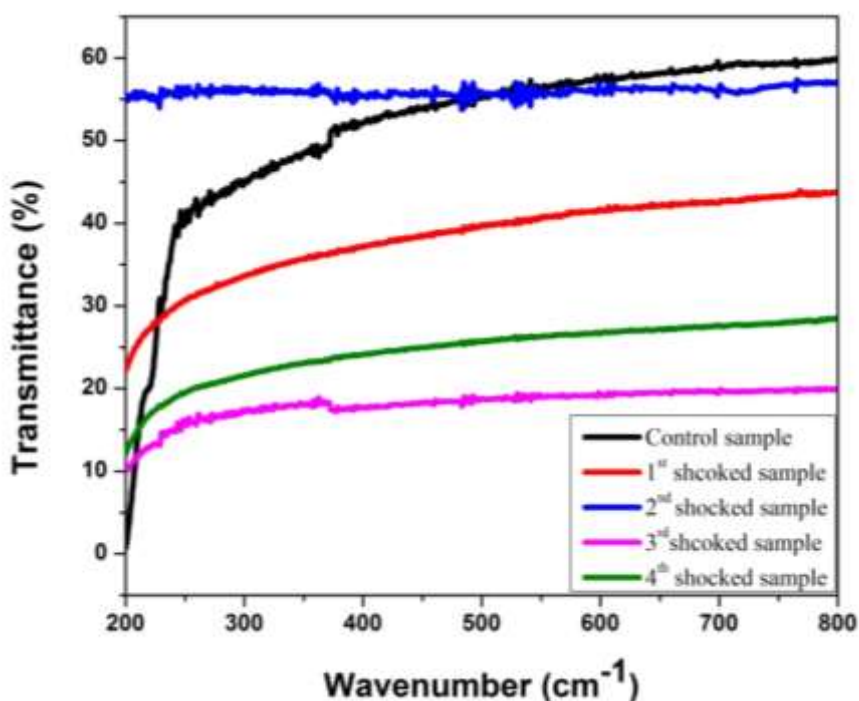


Fig.10 Optical transmittance spectra of the control and shocked samples

As seen in Fig.10, the control test crystal has the absorption edge at 240 nm and it has the optical transmittance value of 59.5% at 800 nm. The appearance of the sharp absorption edge and high optical transmittance illustrate that the control test crystal has good crystalline long-range order crystals. At the 1<sup>st</sup> shocked condition, the optical transmittance is dropped from 59.5% to 43.3% at 800 nm and the absorption edge shift is towards lower wavelength which may be due to the re-organization of hydrogen bonds, re-orientation of crystallographic planes and formation of defected CdO<sub>6</sub> octahedral.<sup>22</sup> At the second shocked condition, the disappearance of the sharp absorption edge of the test crystal is witnessed and its corresponding optical transmittance spectrum is presented in Fig.10 wherein the disappearance of the absorption edge pattern may be due to the formation of the amorphous phase. Indeed, this is one of the few optical properties of crystals which can be taken into the account to justify the short range order and long range order of crystals. It could be noted that, if the test crystal's long range order is destroyed, the sharp band disappears which is typical for short range and amorphous materials.<sup>54,55</sup> Surprisingly, again at the 3<sup>rd</sup> and 4<sup>th</sup> shocked conditions, the appearance of absorption edge at lower wave length regions is visualized. In addition to that, the values of optical transmittance are varied at the 3<sup>rd</sup> and 4<sup>th</sup> shocked conditions and the observed optical transmittance spectra are presented in Fig.10. As seen in Fig.10, at the 3<sup>rd</sup> shocked condition, the test crystal has 28% optical transmittance and 19 % for the 4<sup>th</sup> shocked condition of the crystal. The observed maximum reduction of the optical transmittance for the 4<sup>th</sup> shocked crystal may be due to the presence of minor diffraction planes in the crystal. Hence,

on the one hand, the net concentration of grains might have increased such that it resists the optical transmittance of the test crystal.<sup>49,50</sup> On the other hand, the test crystal's octahedral and tetrahedral sites and their bond lengths as well as bond angles might have been significantly altered with respect to the number of shock pulses. Followed by these changes, the electron density around transition metal cations might have been affected as and when some of the cation octahedra have experienced the highly orientational disorder that could have enlarged the unit cell which could be attributed to the uneven d-electron distribution and as a result, different absorption edge positions have been observed with respect to the number of shock pulse.<sup>54</sup>

## Conclusion

In summarizing the present framework, the switchable phase transition occurring between crystalline and amorphous nature of cadmium sulfate octahydrate single crystal has been systematically presented and demonstrated by employing shock waves and the results have been authenticated by utilizing XRD, Raman and UV-Visible spectral analyses. Diffraction results clearly show the re-orientational changes occurring at the 1<sup>st</sup>, 3<sup>rd</sup>, and 4<sup>th</sup> shocked conditions sustaining the same crystallographic phase (*C2/c*) whereas at the 2<sup>nd</sup> shocked condition, the phase of amorphization exists which is clearly confirmed by the disappearance of all diffraction peaks as observed in the XRD spectra. The phase transition sequence of the test crystal is C-C-A-C-C (C-crystal, A-amorphous) with respect to the control, one, two, three and four shocked conditions. The spectroscopic results of Raman and UV-Visible spectral analyses have been found fairly substantiating the diffraction results with respect to the number of shock pulses and the observed changes are highly associated with re-organization of hydrogen bonds, breaking of lattice symmetry and re-crystallization process. In Raman spectra, Raman bands of sulfate ion and hydrogen bonds undergo Raman peak shifting and disappearance of the absorption edges which are prominent supporting evidence for the diffraction results proving the amorphization occurring at the 2<sup>nd</sup> shocked condition. It could be noted that, at shocked conditions, there is a specific signature found for lower hydrate forms of the test crystal which categorically indicates that the de-hydration process does not occur at shocked conditions even though it has sufficient pressure and temperature. The switching of phase transition occurring between crystalline and amorphous states in materials are highly required for the applications of molecular switching, data storage, dielectric switching, phase shifters, thermo-nuclear devices and current flash memories.

## Acknowledgment

The authors thank Department of Science and Technology (DST), India for funding through DST-FIST programme (SR/FST/College-2017/130 (c)). The project was supported by Researchers Supporting Project number (RSP-2021/231), King Saud University, Riyadh, Saudi Arabia.

### Competing financial interests

The authors declare no competing financial interests.

### References

- [1] Zhi Su, William L. Shaw, Yu-Run Miao, Sizhu You, Dana D. Dlott, and Kenneth S. Suslick, *J. Am. Chem. Soc.* 139 (2017) 4619–4622.
- [2] P. Renganathan and Y. M. Gupta, *J. Appl. Phys.* 126, (2019) 115902.
- [3] Xuan Zhou, Yu-Run Miao, William L. Shaw, Kenneth S. Suslick, and Dana D. Dlott, *J. Am. Chem. Soc.* 141 (2019) 2220–2223.
- [4] Zheng-Hua He, Jun Chen, Guang-Fu Ji, Li-Min Liu, Wen-Jun Zhu, and Qiang Wu; *J. Phys. Chem. B.*, 119 (2015) 10673–10681.
- [5] Shamal L. Chinke, Inderpal Singh Sandhu, D. R. Saroha, and Prashant S. Alegaonkar, *ACS Appl. Nano Mater.* 1 (2018) 6027–6037.
- [6] S. Kalaiarasi, A. Sivakumar, S.A. Martin Britto Dhas, M. Jose, *Mater. Lett.* 219 (2018) 72–75.
- [7] V. Jayaram, K. P. J. Reddy, *Adv. Mater. Lett.* 7 (2016) 100-150.
- [8] Shiteng Zhao, Bimal Kad, Eric Hahn, Laura Chen, Yekaterina, Opachi, Karren More, Bruce Remington, Christopher Wehrenberg, Jerry LaSalvia, Wen Yang, Haocheng Quan, and Marc Meyers. *EPJ Web of Conferences.* 183 (2018) 03027.
- [9] Shiteng Zhao, Bimal Kad, Christopher E. Wehrenberg, Bruce A. Remington, Eric N. Hahn, Karren L. More, and Marc A. Meyers, *Proc Natl Acad Sci.*, 2017, 114, 9791–9796.
- [10] S. J. Wang, M. L. Sui, et al, *Sci. Rep.*, 3 (2013) 1086.
- [11] Nina Gunkelmann, Eduardo M. Bringa, and Herbert M. Urbassek, *J. Appl. Phys.*, 118, (2015) 185902.
- [12] K.D. Joshi, N. Suresh, G. Jyoti, S.K. Kulshreshtha, S.C. Gupta, S.K. Sikka, *Shock Waves.*, 8 (1998) 173–176.
- [13] L. Leiserowitz and G. M. J. Schmidt, *J. Phys. Chem. Solids.*, 27, (1966) 1453-1457.
- [14] Lei Kang, Kai Wang, Shourui Li, a Xiaodong Li and Bo Zou. *RSC Adv.* 5 (2015) 84703-84710.
- [15] Xiaoli Huang, Da Li, et al., *J. Phys. Chem. C.*, 116 (2012) 9744–9749.

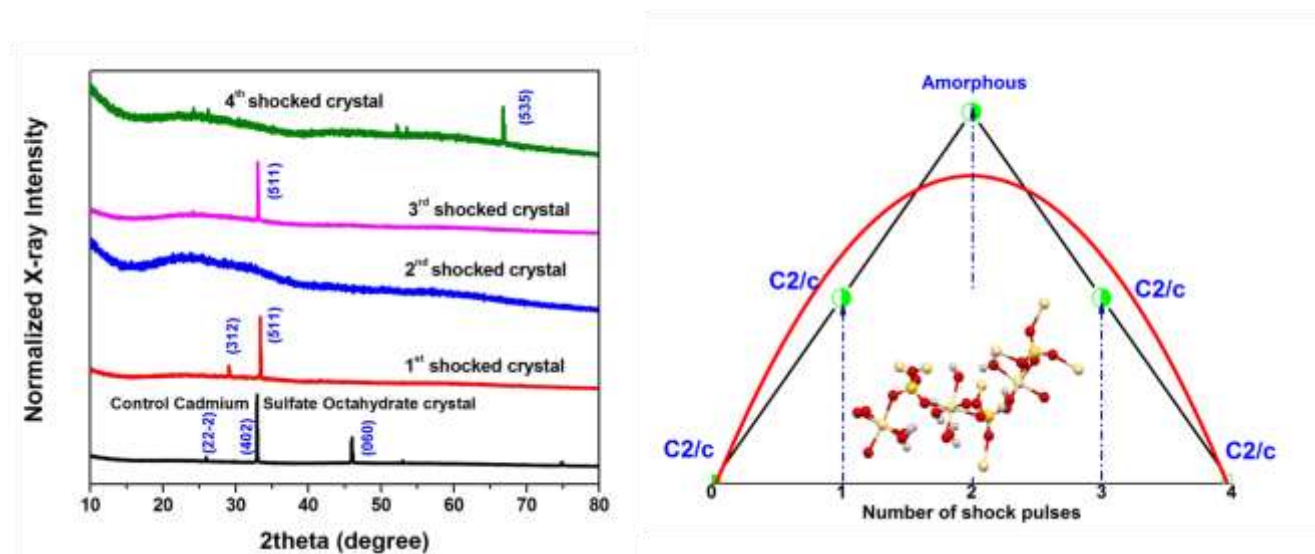
- [16] Lei Kang, Kai Wang, Shourui Li, Jing Liu, Ke Yang, Bingbing Liu, and Bo Zou, *J. Phys. Chem.C*, 118 (2014) 8521–8530.
- [17] Jian Hao, Bo Zou, Pinwen Zhu, Chunxiao Gao, Yinwei Li, Dan Liu, Kai Wang, Weiwei Lei, Qiliang Cui, Guangtian Zou, *Solid. State. Commun.* 149 (2009) 689–692.
- [18] Kwang Soo Lim, Jeong Hwa Song, Dong Won Kang, Minjung Kang, Sunhwi Eom, Eui Kwan Koh, and Chang Seop Hong. *Dalton Trans.*, , 47 (2018) 845-851.
- [19] Lei Wang, Wang Ren, Jing Wen and Bangshu Xiong, *Nanomaterials* 8, (2018) 772.
- [20] Jurepan Piromchom , Nanthawat Wannarit , Jaursup Boonmak, Kittipong Chainok , Chaveng Pakawatchai, Sujittra Youngme, *Inorg. Chem. Commun.* 44 (2014) 111–113.
- [21] A. Sivakumar, S.Reena Devi, S. Sahaya Jude Dhas, R. Mohan Kumar, K.Kamala Bharathi, and S. A. Martin Britto Dhas, *Cryst. Growth Des.*, 20, (2020) 7111–7119.
- [22] A. Sivakumar, S. Soundarya, S. Sahaya Jude Dhas, K. Kamala Bharathi, and S. A. Martin Britto Dhas; *J.Phys.Chem.C* 124, (2020) 10755–10763.
- [23] V. Mowlika, A. Sivakumar, S. A. Martin Britto Dhas, C. S. Naveen, A. R. Phani, R. Robert, *J. Nanostruc.Chem* 10 (2020) 203–209.
- [24] A. Rita, A. Sivakumar, S. Sahaya Jude Dhas, and S. A. Martin Britto Dhas; *J Mater Sci: Mater Electron.*, 31 (2020) 20360–20367.
- [25] I-Ming Chou, Robert R. Seal, Alian Wang., *J. Asian Earth Sci.*, 62, (2013) 734–758.
- [26] Elizabeth C. Sklute, A. Deanne Rogers, Jason C. Gregerson , Heidi B. Jensen , Richard J. Reeder, M. Darby Dyar. *Icarus* 302, (2018) 285–295.
- [27] Encarnacio ´n Ruiz-Agudo, J. Daniel Marti ´n-Ramos, and Carlos Rodriguez-Navarro, *J. Phys. Chem. B* 111, (2007) 41-52.
- [28] Pim A.J. Donkers, Steffen Beckert, Leo Pel, Frank Stallmach, Michael Steiger, and Olaf C.G. Adan, *J. Phys. Chem. C.*, 119, (2015) 28711–28720.
- [29] David T. Vaniman, David L. Bish, Steve J. Chipera, Claire I. Fialips, J. William Carey & William C. Feldman, *Nature.*, 431, (2004) 663- 665.
- [30] M. Andiappan, P. Selvarajan and S. Perumal, *J. Chem.Pharmaceutical Res*, 7, (2015) 1001-1007.
- [31] G. Rajadurai, A. Puhaj Raja and S. Pari, *Archives. Appl. Sci. Res* 5, (2013) 247-253.
- [32] H. Lipson; *Proc. R. Soc. Lond. A.*, 156, (1936) 462-470.
- [33] Chatphorn Theppitak and Kittipong Chainok, *Acta Cryst. E.*, 71, (2015) 8–9.
- [34] Linfei Yang, Lidong Dai, Heping Li, Haiying Hu, Meiling Hong and Xinyu Zhang. *Crystals*, 10, (2020) 75.
- [35] Pim A.J. Donkers, Steffen Beckert, Leo Pel, Frank Stallmach, Michael Steiger, and Olaf C.G. Adan, *J. Phys. Chem. C* 119 (2015) 28711–28720.

- [36] Larysa Okhrimenko, Loic Favergeon, Kevyn, Johannes, Frederic Kuznik, Michele Pijolat, *Thermochim. Acta* 656 (2017)135-143.
- [37] A. Sivakumar, S. Balachandar, S. A. Martin Britto Dhas, *Hum. Fact. Mech. Eng. Defense. Safety.* 4, (2020) 3.
- [38] A.Sivakumar, S.Sahaya Jude Dhas, S.Balachandar, and Martin Britto Dhas; *Z. Kristallogr.* 234, (2019) 557–567.
- [39] Ruggero Caminiti, Georg Jahansson; *Acta.Chemica.Scandinavica A.* 35 (1981) 451-455.
- [40] A. Sivakumar, S.Sahaya Jude Dhas, S.Balachandar, and S.A.Martin Britto Dhas; *J.Elect.Mater.* 48, (2019)7868–7873.
- [41] F.A.I. El-Kabbany, *Phys.Stat. Sol.* 68, (1980) 373.
- [42] Byoung-Koo Choi, Young-Hee Cho And Hyo-Kyoung Lee, *J.Phys.Chem.Solids.*, 54 (1993) 197-201.
- [43] Shiteng Zhaoa, Bimal Kada, Bruce A. Remingtonb, Jerry C. LaSalviac, Christopher E. Wehrenbergb, Kristopher D. Behlerc, and Marc A. Meyers, *Proc Natl Acad Sci.*, 113, (2016) 12088–12093.
- [44] W. Braue, B. Hildmann, H. Schneider, U. Hornemann, *J. Eur. Ceram. Soc.*, 29, (2009) 3135–3146.
- [45] A. Sivakumar, S. Sahaya Jude Dhas, P. Sivaprakash, Abdulrahman I. Almansour, Raju Suresh Kumar, Natarajan Arumugam, S. Arumugam and S. A. Martin Britto Dhas. *New.J.Chem.*, 45 (2021)16529.
- [46] Ray L. Frost and Silmarilly Bahfenne; *J.Raman Spectrosc.* 42, (2011) 219–223.
- [47] P.N.Nandi, D.A. Deshpande, V.G.Kher; *Proc.Indian Aca. Sci.-Chem.Sci.* 88, (1979) 113.
- [48] Alian Wang, John F. Freeman, Bradley L. Jolliff, and Raymond E. Arvidson, *Lunar and Planetary Science XXXVII* (2006)
- [49] A. Sivakumar, S. Sahaya Jude Dhas, S. A. Martin Britto Dhas; *J.Mater.Sci: Mater.Electron.*, 31, (2020) 13704–13713.
- [50] A.Sivakumar, P.Eniya, S.Sahaya Jude Dhas,J. Kalyana sundar, P.Sivaprakash, S.Arumugam and S.A.Martin Britto Dhas; *Z. Kristallogr.*, (2020) DOI: <https://doi.org/10.1515/zkri-2020-0017>
- [51] A.Sivakumar, A.Saranraj, S.Sahaya Jude Dhas, M.Jose, K.Kamala Bharathi, and S.A. Martin Britto Dhas, *Opt.Eng.*, 58, (2019) 107101.
- [52] A.Sivakumar, A. Saranraj, S.Sahaya Jude Dhas, M.Jose and S A. Martin Britto Dhas; *Opt.Eng* 58, (2019) 077104.
- [53] A. Sivakumar, A. Rita, S. Sahaya Jude Dhas, S.A. Martin Britto Dhas, *Optic.Laser. Technol.*, 128, (2020) 106235.

[54] C. Ghosh and B.P. Varma; Solid.State. Commun., 31, (1979) 683-686.

[55] Antony S. Dimitrov, Tetsuya Miwa, and Kuniaki Nagayama, Langmuir., 15, (1999) 5257-5264.

### Journal's Table of Contents (ToC):



### Synopsis

Switchable phase transition from crystal – amorphous states of cadmium sulfate octahydrate (CdSO<sub>4</sub>.8H<sub>2</sub>O) single crystal by shock waves is achieved at ambient condition. The switching of phase transition occurring between crystalline and amorphous states in materials are highly required for the applications of molecular switching, data storage, dielectric switching, phase shifters, thermo-nuclear devices and current flash memories.